2020 DIE CASTING CONGRESS &TABLETOP
NADCA
NORTH AMERICAN DIE CASTING ASSOCIATION

Thermodynamic Modeling and Experimental Investigation of Refractory Materials Used in Aluminum Die Casting

E. Cinkilic, M.P. Moodispaw, A.A. Luo
The Ohio State University, Columbus, OH, USA

Y. Chu
Ryobi Die Casting, Shelbyville, IN, USA

P. Brancaleon
North American Die Casting Association, Arlington Heights, IL, USA

ABSTRACT

Al_2O_3-SiO_2 based refractory materials have been traditionally used in aluminum melting and holding furnaces. However, the formation of corundum (hard, crystalline type of Al_2O_3) has been an issue for these refractories, causing increased downtime due to cleaning operations and reduced energy efficiency in melt processing operations due to the degradation of insulating properties of the refractories. In this study, the thermodynamic stability of common refractory oxides (Al_2O_3, SiO_2, CaO, P_2O_5, ZrO_2, and TiO_2) and antiwetting components was investigated using CALPHAD (CALculation of PHAse Diagrams) modeling tools, in relation to major alloying/impurity elements (Al, Si, Mg, Cu, Fe, Mn, Zn etc.) in aluminum die casting alloys. Based on the thermodynamic simulations, three different refractory materials were selected for melt immersion experiments in atmospheric conditions to validate the simulation results and evaluate the corrosion properties of the refractories of different compositions. The study suggests that replacing SiO_2 with moderate contents of CaO and using combination of Ba-based non-wetting agents as binder can improve the corrosion resistance of refractories significantly.

INTRODUCTION

The corrosion of refractories used in aluminum melting and holding furnaces is a major problem that increases downtime and reduces energy efficiency[1]. The corrosion mainly occurs at the melt line as a result of the reaction between molten aluminum alloy and refractory oxides to generate corundum and elemental silicon. The corundum build-up on the refractory surface can significantly reduce furnace capacity. Therefore, it is required to remove corundum either mechanically or using wall-cleaning fluxes which may damage the refractory surface that will reduce the insulating properties of the refractory, and thus the furnace efficiency.

The corrosion resistance of a refractory depends on its reactivity to molten Al and alloying elements, molten flux and Al_2O_3 in the dross. The refractories based on alumina (Al_2O_3)-silica (SiO_2) system is commonly used due to their low cost and availability. High alumina (60-85% Al_2O_3) refractories are generally used at the melt line of aluminum melting and holding furnaces where they are in direct contact with molten aluminum and dross[1]. These refractories mainly contain corundum (Al_2O_3), silica (SiO_2) and/or their combined form of mullite ($Al_6Si_2O_{13}$). Free SiO_2 or its complex form mullite present in these refractories is attacked by molten aluminum which lead to degradation of mechanical and insulating properties of refractories[2,3].

The corrosion resistance of refractories is generally improved by additions of non-wetting agents to limit melt-refractory interactions. Barite ($BaSO_4$)[4–6], fluorspar (CaF_2)[7], aluminum fluoride (AlF_3)[7], wollastonite ($CaSiO_3$)[1], and B-based compounds[8] were used to improve non-wetting properties. Non-wetting additives react with main components of refractories and molten aluminum to form complex compounds such as hexa-celsian ($BaAl_2Si_2O_8$)[4], aluminum borate ($Al_{18}B_4O_{33}$) that reduce wettability of refractory, and therefore penetration of metal through the refractory surface that improve its corrosion resistance.

Development of better refractories can be achieved by understanding interactions of aluminum with its alloying elements with main refractory components and additives. The CALculation of PHAse Diagrams (CALPHAD) approach has been successfully used for development of new materials for wide range of applications through better understanding of thermodynamics of complex material systems. Application of CALPHAD methodology to investigate the thermodynamics of reactions between molten aluminum and refractory components can provide valuable insights for developing more corrosion resistant refractories through optimization of composition and processing conditions.

In this study, a systematic thermodynamic simulation of refractory materials was conducted. The possibility of any reaction between an alloying element and a refractory component was evaluated by means of Gibbs free energy of formation. Based on the simulation results, representative refractories were selected to perform immersion experiments and characterize molten metal-refractory interface for validation.

THERMODYNAMIC SIMULATIONS AND IMMERSION EXPERIMENTS

THERMODYNAMIC SIMULATIONS

Thermodynamic simulations were performed using ThermoCalc 2020a software with SSUB6 Substances Database, v6[9]. A list of possible reaction paths for each alloying element and refractory component were simulated for a temperature range from room temperature to 1800°C at every 100°C increment. Relative stability of oxides that are used as main refractory components and non-wetting agents were evaluated based on calculated Gibbs free energy of formation. For example, if the calculated Gibbs free energy of formation for an element-oxide couple has a negative value within the temperature range that covers aluminum melting operations, it means that the alloying element tends form its oxide in the expense of the oxide that is the refractory component, and thus, corrosion would take place.

IMMERSION EXPERIMENTS

To evaluate the corrosion properties of selected refractories, immersion experiments were performed. Test bars with dimensions of 1/2”x1/2”x4” were cut from refractory bricks and placed into a crucible with 100g of EZCast alloy (Al-8.5Si-0.35Mg-0.6Mn-0.02Sr). The crucible was loaded into a muffle furnace and heated to 675°C (1250°F). After the alloy is molten, surface dross was cleaned, and samples were kept in the furnace under atmospheric conditions for 100hrs. The samples were cooled in the furnace to allow alloy to solidify around the refractory to maintain the interface. Then, samples were cut in half using an abrasive saw for characterization of interactions between molten alloy and refractory.

SCANNING ELECTRON MICROSCOPY (SEM) CHARACTERIZATION

Immersion test samples were cut after the melt tests were subjected to scanning electron microscopy (SEM) characterization. Combination of zirconia and SiC abrasive papers were used for rough grinding followed by fine polishing with diamond solutions and colloidal silica. These samples were characterized by SEM under low vacuum conditions and using back-scattered imaging mode. Interfaces of immersion test samples were characterized by performing elemental mapping using an energy dispersive X-ray EDX system.

RESULTS AND DISCUSSION

The compositions of refractories from various suppliers were surveyed. The commercial refractories are mainly composed of Al_2O_3, SiO_2, CaO and low levels of P_2O_5, ZrO_2, and TiO_2. The stability of common refractory oxides (Al_2O_3, SiO_2, CaO, P_2O_5, ZrO_2, and TiO_2) respect to the major alloying/impurity elements (Al, Si, Mg, Cu, Fe, Mn, Zn etc.) were investigated using CALPHAD modeling tools. The changes in Gibbs free energy of formation for elemental oxide formation in the expense of refractory components are presented in Figure 1 for Al_2O_3, SiO_2, CaO and P_2O_5. Based on the simulation results, Al_2O_3 and SiO_2 are both attacked by Mg and Sr (Figures 1a and b). In addition, SiO_2 is also attacked by Al to form Al_2O_3. On the other hand, CaO does not interact with any of the common alloying elements. P_2O_5 is reported to be present in some of the commercial refractories and complex phosphate compounds were used as binder in castable refractories. At melting temperatures of aluminum alloys, P_2O_5 reacts with Al, Si, Mn, Zn, Mg and Sr to form oxides these alloying elements.

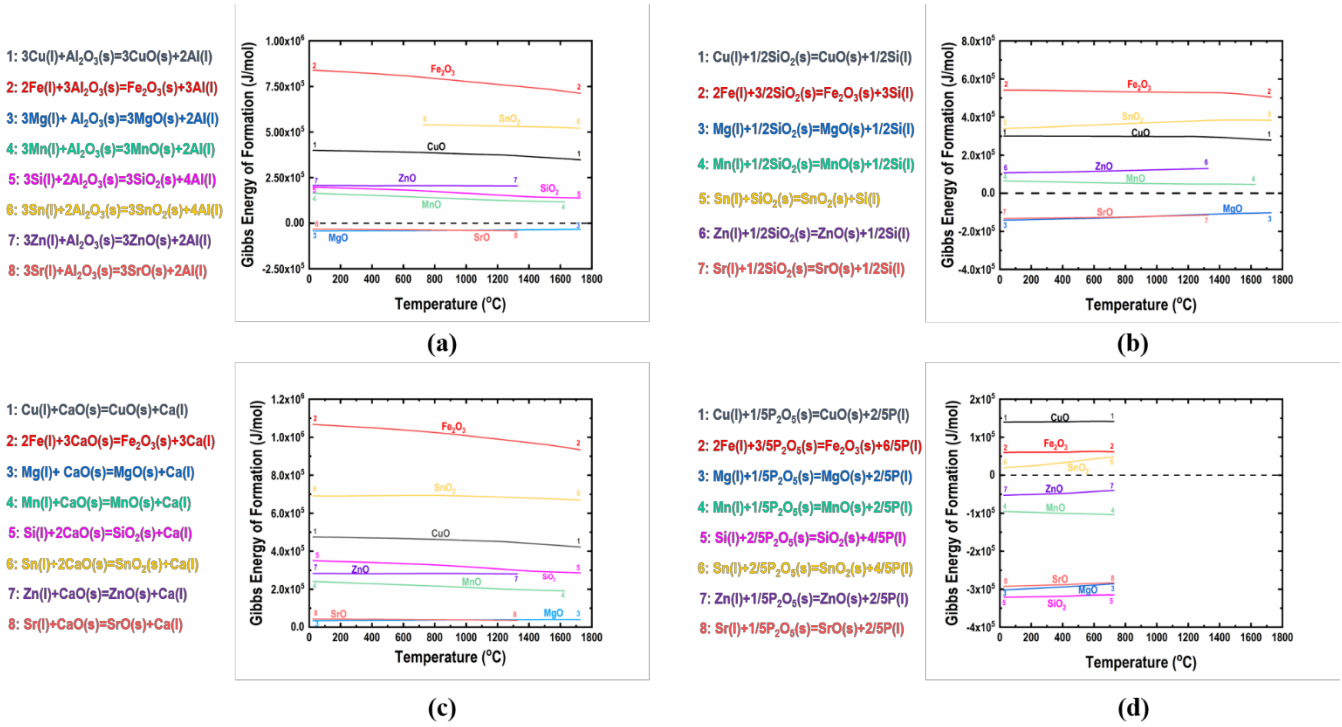

Figure 1- Calculated Gibbs free energy of formation for oxides of different alloying elements in expense refractory components, (a) x-Al_2O_3, (b) x-SiO_2, (c) x-CaO, and (d) x-P_2O_5.

Table 1 Summary of simulation results for element-oxide interactions that were selected based on survey on composition of commercial refractories.

	Al	*Si*	*Cu*	*Fe*	*Mn*	*Zn*	*Sn*	*Mg*	*Sr*	*Evaluated Reactions*
Al_2O_3	***N/A***	✗	✗	✗	✗	✗	✗	✔	✔	$X+2/3Al_2O_3=XO_2+4/3Al$ (X= Si, Sn) $X+1/3Al_2O_3=XO+2/3Al$ (X= Cu, Mn, Zn, Mg, Sr) $2X+Al_2O_3=X_2O_3+2Al$ (X= Fe)
SiO_2	✔	***N/A***	✗	✗	✗	✗	✗	✔	✔	$X+SiO_2=XO_2+Si$ (X= Si, Sn) $X+1/2SiO2=XO+1/2Si$ (X= Cu, Mn, Zn, Mg, Sr) $2X+3/2SiO_2=X2O3+3/2Si$ (X= Fe)
CaO	✗	✗	✗	✗	✗	✗	✗	✗	✗	$X+2CaO=XO_2+2Ca$ (X= Si, Sn) $X+CaO=XO+Ca$ (X= Cu, Mn, Zn, Mg, Sr) $2X+3CaO=X_2O_3+3Ca$ (X= Fe)
P_2O_5	✔	✔	✗	✗	✔	✔	✗	✔	✔	$X+2/5P_2O_5=XO_2+4/5P$ (X= Si, Sn) $X+1/5P_2O_5=XO+2/5P$ (X= Cu, Mn, Zn, Mg, Sr) $2X+3/5P_2O_5=X_2O_3+3/5P$ (X= Fe)
ZrO_2	✗	✗	✗	✗	✗	✗	✗	✔	✔	$X+ZrO_2=XO_2+Zr$ (X= Si, Sn) $X+1/2ZrO2=XO+1/2Zr$ (X= Cu, Mn, Zn, Mg, Sr) $2X+3/2ZrO_2=X_2O_3+3/2Zr$ (X= Fe)
TiO_2	✔	✗	✗	✗	✗	✗	✗	✔	✔	$X+TiO_2=XO_2+Ti$ (X= Si, Sn) $X+1/2TiO_2=XO+1/2Ti$ (X= Cu, Mn, Zn, Mg, Sr) $2X+3/2TiO_2=X_2O_3+3/2Ti$ (X= Fe)
✔: Reaction possible, ✗: Reaction not possible										

Thermodynamic calculations were performed for oxides with more than 1% presence in commercial refractories. The summary of simulation results is presented in Table 1. All the oxides listed, except for CaO, can react with Mg and Sr. In addition to Mg and Sr, Al can also react with SiO_2, P_2O_5, and TiO_2 to form Al_2O_3. These simulation results are consistent with in-plant observations of corundum (Al_2O_3) and spinel ($MgO.Al_2O_3$) build-up on the holding furnaces at Ryobi Die Casting plant, Shelbyville, IN. One may think that refractories are primed or fired at high temperatures and can yield complex oxides of these individual components. For example, mullite ($3Al_2O_3 \cdot 2SiO_2$ or $Al_6Si_2O_{13}$) formation occurs at firing temperatures above 1000°C in high-alumina refractories. A similar thermodynamic analysis yields that mullite reacts with alloying elements in a similar way as SiO_2 and still interacts with Mg, and Sr to form MgO and SrO within the investigated temperature range. This implies that complex oxides of main components may behave similarly to their individual components. These simple thermodynamic calculations suggest that Al_2O_3-CaO based refractories are more resistant to corrosion.

To validate the thermodynamic simulation results, three commercial refractories were selected from a list of available products for evaluation based on refractory composition (Table 2). Specifically, the composition was selected to evaluate the effect of replacing SiO_2 by CaO to increase the corrosion resistance of refractory materials. R1is a high Al_2O_3/SiO_2 ratio refractory with low content of CaO. It is a low cement refractory with Al non-wetting properties. R2 and R3 are both SiO_2 free and contains CaO in the form of calcium aluminate (Al_2CaO_4). Another component in R2 and R3 is $BaSO_4$ which is known to be an effective non-wetting agent. However, the information on non-wetting component used in R1 is not known.

Table 2 The composition of selected refractories used in immersion experiments.

	Al_2O_3	SiO_2	CaO	TiO_2	Fe_2O_3	MgO	P_2O_5	$BaSO_4$	Ka_2O	Na_2O	SiC	ZrO_2	Others
R1	83.8	8.9	2.0	0.9	0.4				0.1	0.1			3.8
R2	78.6	0.7	10.5	0.1	0.1	0.1		10					10
R3	64.6	0.3	24.3	0.1	0.1	0.2		10					10

Immersion experiments were performed to evaluate the corrosion properties under air. An example of immersion test sample and back-scattered SEM image of refractory-metal interface at the metal line is presented in Figure 2 for R1 and EZCast alloy. An interaction layer between refractory and molten metal is observed at the metal line. On the other hand, away from the metal line towards the bottom of the melt pool, there was no interaction.

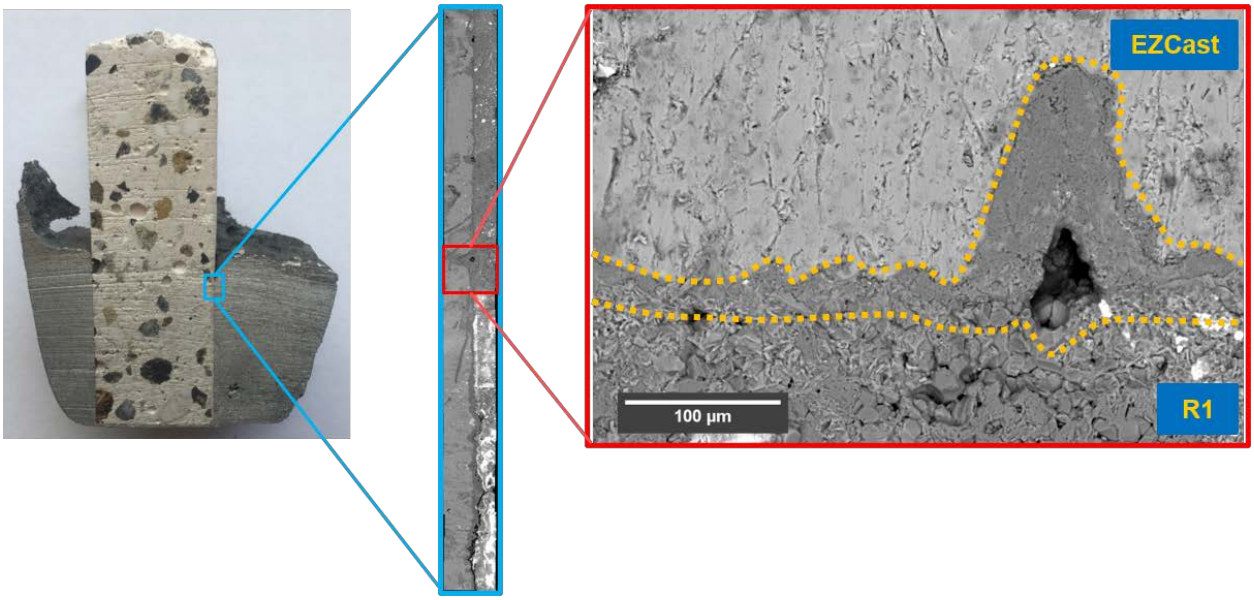

Figure 2- Immersion experiment sample and associated microstructure image obtained from metal line.

Figure 3 shows typical back-scattered SEM images for the tested refractories. In Figure 3a, an interaction layer with a thickness of ~20 microns between EZCast and R1 was observed. The thickness of the interaction layer varies, and a bulge was grown on the refractory into the molten metal. The interaction between EZCast and R2 is minimal at the metal line (Figure 3b). Large calcium aluminate (Al_2CaO_4) particles were wetted by the melt when they were at the interface and in direct contact with molten aluminum. On the other hand, a mixture of fine Ba-based and Ca-based particles did not interact with the molten metal. In Figure 3c, it can be seen that EZCast interacted with R3 at the metal line and formed a thick interaction layer. The microstructure of R3 is different from R2 which shows limited interaction with the EZCast alloy.

Figure 4 presents a comparison of composition analysis results of interface layers between the refractories and EZCast. The distribution of main elements at the interface is evaluated. The interaction layer observed between EZCast and R1 is mainly composed of Mg, Al, and O, which is consistent with corundum and spinel formation observed on refractories used in melting and holding furnaces (the left set of images in Figure 4). The EZCast-R2 interface shows that large calcium aluminate particles are in direct contact with molten aluminum in addition to barite and Ca-based cement mixture (Figure 4, the middle set of images). It can be seen from compositional analysis that Mg interacts with large calcium aluminate particles and penetrate further into the refractory through these particles. In contrast, only a thin Mg rich layer was formed on the barite and Ca-based cement mixture and no penetration was observed. In the right set of images in Figure 4, the interaction layer again mainly consists of Mg, Al, and O. No penetration into the refractory was observed, but an interaction layer with uniform thickness of ~25 microns was formed. In addition to Mg, Al, and O, Ca is not present in the interaction layers of R3 and R2 samples which suggest that CaO is not reacting with molten aluminum alloy. This is consistent with the thermodynamic simulation results.

There are stark differences in microstructure of R2 (Figure 3b) and R3 (Figure 3c) refractories, which are responsible for distinct interaction behavior with molten aluminum. Each refractory contains same amount of barite and different contents of CaO. Based on thermodynamic calculations and immersion experiments, it is clear that CaO is non-reacting with molten aluminum and its major alloying elements. The difference is mainly due to how barite, a non-wetting component, is employed to improve the corrosion properties. As it can be seen from the back-scattered SEM images, R2 mainly consists of large calcium aluminate (Al_2CaO_4) particles which were bound with a mixture of fine particles mainly composed of Ba, Al, Ca, S and O. These particles are most likely a mixture of $BaSO_4$, Al_2BaO_4 and CaO. These compounds do not interact with any major alloying elements based on thermodynamic simulations and no interaction layer was observed where they are in direct contact with molten aluminum. A reaction path for the formation of Al_2BaO_4 compound involves decomposition of $BaSO_4$ into BaO, according to reaction at firing temperature of 1200°C:

$$2BaSO_{4(s)} \rightarrow 2BaO_{(s)} + 2SO_{2(g)} + O_{2(g)}$$

followed by:

$$BaO_{(s)} + Al_2CaO_4 \rightarrow Al_2BaO_{4(s)} + CaO_{(s)}$$

These transformation reactions are crucial to improve corrosion properties of the refractory, since barite and calcium aluminate react with Al, Mg, and Sr according to the thermodynamic simulations. In addition to the thermodynamic aspect of corrosion behavior, the physical properties of refractory components are also important. As in the case of R3, large particles of Al_2BaO_4.CaO were still formed. However, the surface area of these particles is significantly smaller compared to ones in R2 and therefore they do not interact with molten aluminum and major alloying elements as much. Instead for R3 is composed of a mixture of refined calcium aluminate particles surrounded by Al and Ca-rich cement which can be wetted and penetrated by molten aluminum when it is in direct contact.

Both R3 and R2 samples contain very small amount of silica (SiO_2). According to literature, additions of micro silica in presence of Ba-containing non-wetting agents can improve the corrosion resistance due to the formation of hexa-celsian ($BaAl_2Si_2O_8$)[4–6]. However, in case of CaO containing refractories, the presence of micro-silica can lead to formation of another compound called anorthite ($CaAl_2Si_2O_8$) which can be attacked by Mg, Zn and Sr according to the thermodynamic simulations and literature data[10,11]. Optimization of micro-silica content and firing temperature can further improve the corrosion properties of R2.

$$2BaSO_{4(s)} + 4SiO_{2(s)} + 2Al_2O_3(s) \rightarrow 2\ BaAl_2Si_2O_{8(s)} + 2SO_{2(g)} + O_{2(g)}$$

$$Al_2CaO_{4(s)} + 2SiO_{2(s)} \rightarrow CaAl_2Si_2O_{8(s)}$$

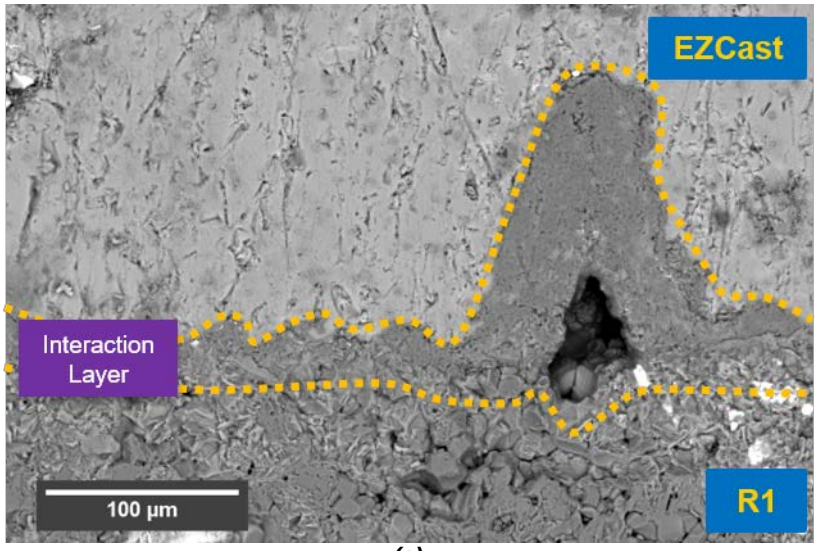

(a)

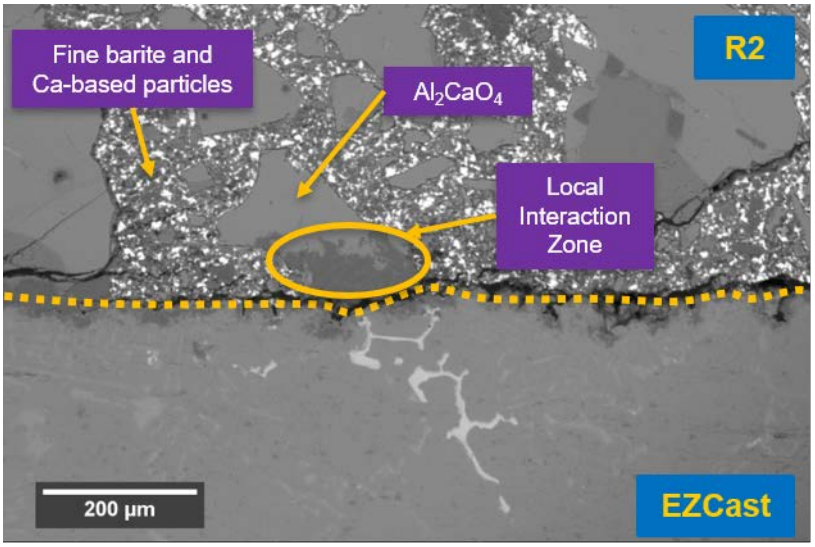

(b)

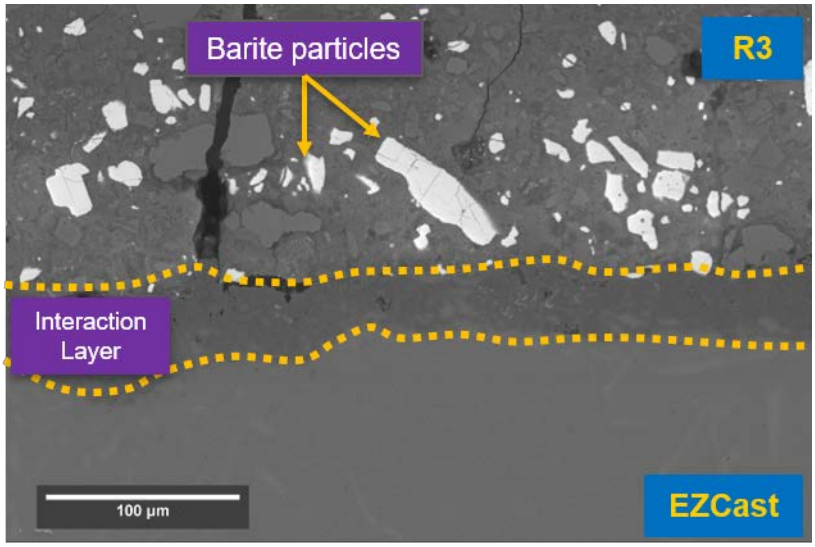

(c)

Figure 3- Interaction layers between refractory and alloy at the metal line

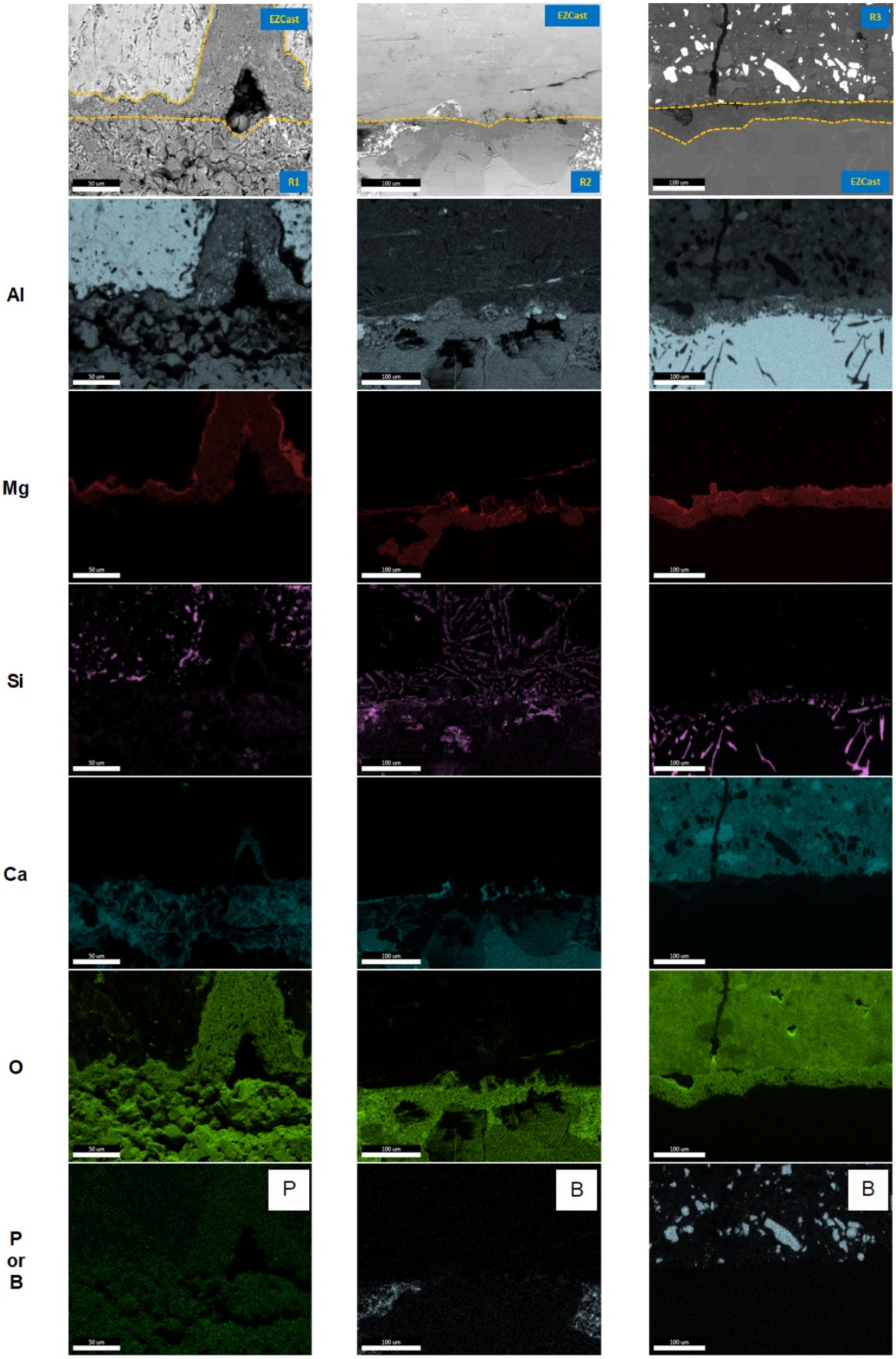

Figure 4- Interaction layers between refractory and alloy at the metal line

CONCLUSIONS

The corrosion properties of several refractories used in aluminum melting and holding furnace operations were investigated using thermodynamic simulations and melt immersion experiments. According to the thermodynamic simulations, Al_2O_3-CaO based refractories can be more resistant to chemical attacks from molten aluminum and its major alloying elements, compared to Al_2O_3-SiO_2 based refractories. This is because SiO_2 is severely attacked by Al, Mg, and Sr when in contact with molten aluminum alloys. Based on the melt immersion experiments, the physical properties of refractory components are proved to be important. The difference in particle sizes of calcium aluminate and barite compound used in Al_2O_3-CaO refractories as non-wetting component can also significantly alter the corrosion behavior of the refractory. As a result, R2 sample consists of large calcium aluminate particles and refined mixture of Al_2BaO_4 and CaO cement showed the best corrosion properties in this study.

ACKNOWLEDGMENTS

This material is based upon work supported by the U.S. Department of Energy's Office of Energy Efficiency and Renewable Energy (EERE) under the Advanced Manufacturing Office Award Number DE-EE0007897.

DISCLAIMER

REFERENCES

1. M.E. Schlesinger: *Aluminum Recycling*, 2nd edn., CRC Press, Boca Raton, FL, 2013.
2. M. Allahevrdi, S. Afshar, and C. Allaire: *JOM*, 1998, vol. 50, pp. 30–4.
3. S. Afshar and C. Allaire: *JOM*, 2001, vol. 53, pp. 24–7.
4. E. AdabiFiroozjaei, P. Koshy, and E. Rastkerdar: *Metall. Mater. Trans. B*, 2011, vol. 42, pp. 901–13.
5. S. Afshar, C. Gaubert, and C. Allaire: *JOM*, 2003, vol. 55, pp. 66–9.
6. P. Koshy, S. Gupta, P. Edwards, and V. Sahajwalla: *J. Mater. Sci.*, 2011, vol. 46, pp. 468–78.
7. S. Afshar and C. Allaire: *JOM*, 2000, vol. 52, pp. 43–6.
8. E. AdabiFiroozjaei, P. Koshy, and C.C. Sorrell: *Metall. Mater. Trans. B*, 2012, vol. 43, pp. 5–13.
9. Thermo-Calc Software SSUB6 Substances Database: 2020.
10. E. Adabifiroozjaei, P. Koshy, E. Rastkerdar, and C.C. Sorrell: *J. Am. Ceram. Soc.*, 2016, vol. 99, pp. 1694–708.
11. E. Adabifiroozjaei, H. Ma, P. Koshy, and C.C. Sorrell: *J. Mater. Sci.*, 2017, vol. 52, pp. 6767–77.